Neuron
Article

Microglial CR3 Activation Triggers Long-Term Synaptic Depression in the Hippocampus via NADPH Oxidase

Jingfei Zhang,[1] Aqsa Malik,[1] Hyun B. Choi,[1] Rebecca W.Y. Ko,[1] Lasse Dissing-Olesen,[1] and Brian A. MacVicar[1,*]
[1]Brain Research Centre, Department of Psychiatry, University of British Columbia, Vancouver, BC V6T 2B5, Canada
*Correspondence: bmacvicar@brain.ubc.ca
http://dx.doi.org/10.1016/j.neuron.2014.01.043

SUMMARY

Complement receptor 3 (CR3) activation in microglia is involved in neuroinflammation-related brain disorders and pruning of neuronal synapses. Hypoxia, often observed together with neuroinflammation in brain trauma, stroke, and neurodegenerative diseases, is thought to exacerbate inflammatory responses and synergistically enhance brain damage. Here we show that when hypoxia and an inflammatory stimulus (lipopolysaccharide [LPS]) are combined, they act synergistically to trigger long-term synaptic depression (LTD) that requires microglial CR3, activation of nicotinamide adenine dinucleotide phosphate oxidase (NADPH oxidase), and GluA2-mediated A-amino-3-hydroxy-5-methyl-4-isoxazolepropionic acid receptor (AMPAR) internalization. Microglial CR3-triggered LTD is independent of N-methyl-D-aspartate receptors (NMDARs), metabotropic glutamate receptors (mGluRs), or patterned synaptic activity. This type of LTD may contribute to memory impairments and synaptic disruptions in neuroinflammation-related brain disorders.

INTRODUCTION

Microglia, the resident immune cells in the brain, are critically involved in neuroinflammation in various pathological conditions, including stroke, trauma, and neurodegenerative diseases (Hanisch and Kettenmann, 2007; Kettenmann et al., 2011). In the healthy brain, microglia exhibit highly motile processes that frequently contact neuronal synapses (Wake et al., 2009) or surround damaged tissue (Nimmerjahn et al., 2005). Recent studies have shown that microglia shape neuronal networks by pruning synapses during development (Kettenmann et al., 2013; Wake et al., 2013) via activation of complement receptor 3 (CR3), a microglia-specific pattern recognition receptor consisting of a cluster of differentiation molecule 11b (CD11b) and CD18 (Stephan et al., 2012). Synaptic pruning probably requires the well-known CR3 ligand complement 3 (Schafer et al., 2012; Stephan et al., 2012; Stevens et al., 2007). However, in addition to complement 3, CR3 also directly recognizes various types of neuroinflammatory stimuli such as lipopolysaccharide (LPS) (Flaherty et al., 1997; Wright and Jong, 1986), β amyloid (Zhang et al., 2011), high-mobility group box 1 (HMGB1) (Gao et al., 2011), α-synuclein (Zhang et al., 2007), and filamentous hemagglutinin of bacteria (Relman et al., 1990), all of which can under some circumstances cause neurotoxicity (Gao et al., 2011; Pei et al., 2007; Zhang et al., 2007, 2011). Therefore, we have investigated the impact of activating CR3 with an inflammatory ligand, LPS, on synaptic function to provide insights into the pathology of neuroinflammation-mediated brain disorders.

Inflammatory neuropathologies, such as stroke, trauma, and neurodegenerative diseases, are often associated with hypoxia from reductions and alterations in neurovascular coupling and cerebral blood flow (Peers et al., 2009; Zlokovic, 2011). Hypoxia can act synergistically with neuroinflammation to enhance damage and precipitate cognitive decline in pathological conditions, although the mechanisms by which hypoxia and inflammation interact in the CNS are still largely unknown (Peers et al., 2009; Zlokovic, 2011). Recent reports have shown that in the peripheral immune system, inflammation and hypoxia share similar downstream pathways resulting in enhanced inflammatory reactions (Nizet and Johnson, 2009; Rius et al., 2008). In this study, we investigated whether hypoxia and an inflammatory stimulus act synergistically to modulate synaptic function via a microglial CR3-dependent mechanism.

RESULTS

LPS and Hypoxia Rapidly Induce Long-Term Synaptic Depression in Both Rats and Mice with a Mechanism that Requires Microglial CR3

In order to investigate the impact of concurrent CR3 activation and hypoxia on synaptic transmission, we recorded field potentials in the CA1 region of hippocampal brain slices from both rats (wild-type [WT]) and mice (WT and CR3 knockout [CR3 KO]) and applied combinations of LPS and a hypoxic stimulus (artificial cerebrospinal fluid [aCSF] aerated with 8% O_2). As shown in Figure 1A, application of only LPS (10 μg/ml) on rat hippocampal slices did not change basal synaptic transmission (n = 6, 101.2% ± 1.6% of baseline). Hypoxia alone (for 15 min) without LPS caused a well-known transient depression of field excitatory postsynaptic potentials (fEPSPs) from adenosine release (Dunwiddie and Masino, 2001), which fully recovered after reperfusion of normal aCSF (n = 6, 103.2% ± 7.5% of baseline 30 min after normoxic reperfusion; Figure 1A). However, when we coapplied 15 min of 8% O_2-aerated aCSF concurrently with LPS, we

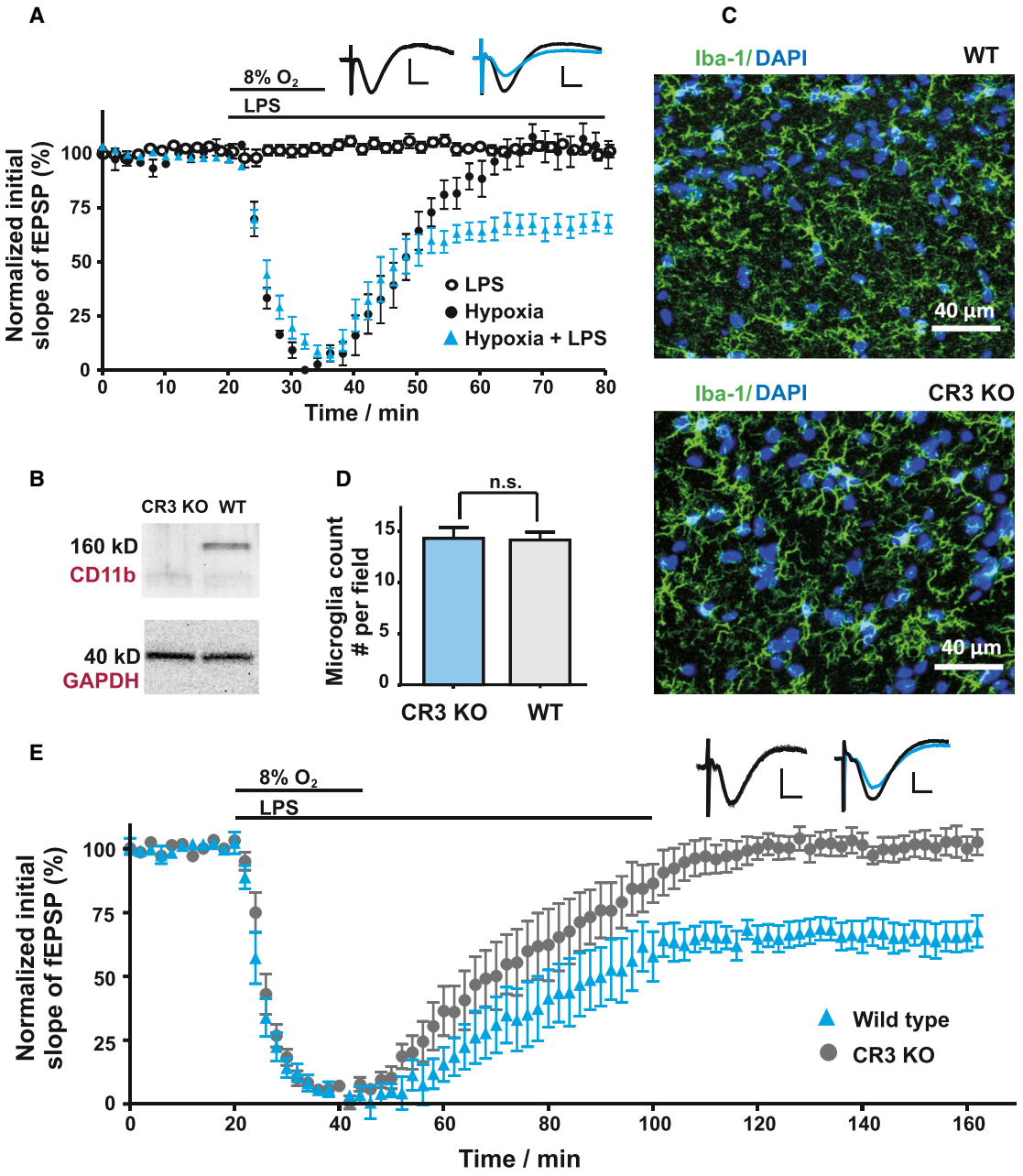

Figure 1. LPS and Hypoxia Induce LTD that Depends on Microglial CR3 Activation

Field recordings were performed in the CA1 area of hippocampal slices.

(A) Perfusion of LPS (10 μg/ml) did not alter basal synaptic transmission; hypoxia (8% O_2-aerated aCSF) caused an immediate transient depression of fEPSP, which was fully reversed after reperfusion of normoxic (95% O_2 saturated) aCSF; when LPS and hypoxia were applied together, an LTD of fEPSP was observed. In all figures, sample traces were taken from the time points when statistics were performed.

(B) Western blot of CD11b in both WT and CR3 KO mice.

(C) Sample images of immunohistostaining of Iba-1 and DAPI staining of nuclei in stratum radiatum of hippocampal CA1 in both WT and CR3 KO mice.

(D) Microglial counts in both WT and CR3 KO mice. Microglia were recognized as Iba-1-positive cells with DAPI-positive nuclei in the middle.

(E) LPS and hypoxia induced LTD in WT mice but not in CR3 KO mice. Scale bars for all sample fEPSP traces in all figures represent 10 ms (horizontal) and 0.5 mV (vertical). All error bars represent SEM.

observed long-term depression (LTD) of fEPSPs with a decrease to 66.8% ± 3.7% of baseline (mean field potentials 30 min after normoxic reperfusion, n = 5, $p < 0.01$ compared to hypoxia-only, Figure 1A). This depression, although not shown in the figure, was observed to be stable at 64.3% ± 7.4% (n = 5) at 75 min after treatment. Our results show that concurrent hypoxia

and LPS application induced LTD in the hippocampus (referred to subsequently as LPS+hypoxia LTD). Furthermore, as shown in Figure S1 available online, increasing the concentration or application time of any one of the stimuli (i.e., doubling concentration of LPS [Figure S1A], 0% instead of 8% O_2 [Figure S1B], or doubling the duration of hypoxia exposure [Figure S1C]) did not induce LTD in rat hippocampal slices, suggesting that the two stimuli act synergistically to induce LTD.

In order to determine whether CR3 is the key receptor mediating LPS+hypoxia LTD, we used CR3 KO mice (lacking subunit CD11b) and WT mice. In the brain, CR3 is expressed exclusively in microglia and CD11b is a well-established and selective microglia marker (Hickman et al., 2013). We confirmed that CD11b and ionized calcium binding adaptor molecule 1 (Iba-1) staining overlapped on the same cells in WT mice (Figure S2A). In hippocampal tissue from CR3 KO mice, CD11b was undetectable by western blots (Figure 1B), and we could see no immunohistochemical staining for CD11b in Iba-1-positive microglia (Figure S2B). In addition, we observed no striking differences in morphology of Iba-1-positive microglial in the hippocampus (CA1 stratum radiatum) from CR3 KO compared to WT mice (Figure 1C). Furthermore, Figure 1D shows that microglial number counts in the CA1 stratum radiatum from WT and CR3 KO are not significantly different (14.2 ± 0.8/field in WT and 14.3 ± 1.1/field in CR3 KO, $p > 0.05$, 18 fields from 3 animals in each group). One field was defined as a stack of 23 images (separated by 1 μm) with dimensions of 212 μm × 212 μm and a total thickness of 22 μm.

In slices obtained from WT mice, LPS (15 μg/ml) applied concurrently with 8% O_2-aerated aCSF for 25 min induced an LTD with a decrease to 65.2% ± 4.6% of baseline (calculated based on mean field potentials 75 min after normoxic reperfusion, n = 6; Figure 1E). However, when we applied the same treatment on slices obtained from CR3 KO mice, LTD was not observed and field potentials recovered to 99.7% ± 4.6% of baseline ($n = 9$, $p < 0.001$ compared to WT mice; Figure 1E). The absence of LTD in CR3 KO mice indicates that LPS and hypoxia induced LTD with a mechanism that requires activation of microglial CR3.

LPS+Hypoxia LTD Is Not Dependent on NMDAR, mGluR, Adenosine Deceptor, or Toll-like Receptor 4

We next explored the pathways downstream of CR3 activation to investigate whether LPS+hypoxia LTD was similar to previously reported types of LTD that require activation of N-methyl-D-aspartate receptors (NMDARs) or metabotropic glutamate receptors (mGluRs) (Collingridge et al., 2010) or adenosine A1 receptors that are activated by adenosine release during hypoxia (von Lubitz, 1999). As shown in Figures 2A and 2B, antagonists of these receptors had no effect on LPS+hypoxia LTD in rat hippocampal slices (60.2% ± 5.3% of baseline in the NMDAR antagonist APV [100 μM], $n = 6$, $p > 0.05$; 68.4% ± 5.7% of baseline in the group I/II mGluR antagonist [(R,S)-α-methyl-4-carboxyphenylglycine (MCPG, 250 μM)], $n = 6$, $p > 0.05$; 73.4% ± 3.2% of baseline in the selective group II mGluR blocker LY341495 [100 μM], $n = 5$, $p > 0.05$; 63.4% ± 3.8% of baseline in the adenosine A1 receptor blocker 8-cyclopentyl-1,3-dipropylxanthine [DPCPX, 500 nM], $n = 6$, $p > 0.05$). These results suggest that LPS+hypoxia LTD is not mediated by NMDAR, mGluR, or A1 receptor activation.

Previous studies have shown that LPS activates microglial toll-like receptor 4 (TLR4) and subsequently blocks the induction of LTP by triggering the release of cytokines in a complex process involving transcription, translation, and synthesis of cytokines (Hauss-Wegrzyniak et al., 2002; Kettenmann et al., 2011; Nolan et al., 2004). To examine the possible participation of the TLR4 pathway, we applied TAT-MyD88 (YGRKKRRQRRR-RDVLPGT), a peptide that blocks the interaction between TLR4 and its adaptor MyD88, therefore inhibiting part of the downstream signaling pathway that produces cytokines (Hines et al., 2013). As shown in Figure 2C, when included in the preincubation (for 1 hr) and perfusion solutions, TAT-MyD88 (1 μM) did not block LPS+hypoxia LTD in rat hippocampal slices, leading to a depression 75.8% ± 2.8% of baseline ($n = 4$, $p > 0.05$ compared to LPS+hypoxia, $p < 0.01$ compared to hypoxia alone). Therefore, our results suggest that the TLR4-induced MyD88-dependent pathway is not essential in LPS+hypoxia LTD.

To further investigate the role of TLR4 activation in LPS+hypoxia LTD, we tested LPS+hypoxia LTD in slices obtained from TLR4 KO mice. LPS (15 μg/ml) applied concurrently with 8% O_2-aerated aCSF for 25 min induced an LTD with a decrease to 65.9% ± 9.3% of baseline 75 min after normoxic reperfusion ($n = 7$, $p > 0.05$ compared to WT mice, and $p < 0.001$ compared to CR3 KO mice; Figure 2D). Taken together, our observations suggest that TLR4 activation does not play a major role in LPS+hypoxia LTD.

LPS+Hypoxia LTD Requires Activation of NADPH Oxidase

Previous studies have reported that the stimulation of microglial CR3 by LPS rapidly activates nicotinamide adenine dinucleotide phosphate oxidase (NADPH oxidase), which produces superoxide that reaches peak levels within 30 min (Pei et al., 2007; Qin et al., 2004). NADPH oxidase, known to play a key role in neurodegeneration (Gao et al., 2012), can be activated by neuroinflammation and hypoxia through distinct pathways (Bedard and Krause, 2007). Therefore, we investigated the possible contribution of NADPH oxidase to LPS+hypoxia LTD. The NADPH oxidase blocker apocynin (100 μM) completely prevented LPS+hypoxia LTD in rat hippocampal slices when coapplied (97.2% ± 4.3% of baseline, $n = 5$, $p < 0.01$ compared to LPS+hypoxia, and $p > 0.05$ compared to hypoxia alone; Figure 3A). When we applied apocynin 15 min after reperfusion of normoxic solution, LPS+hypoxia LTD was still observed (67.8% ± 9.2%, $n = 4$, $p > 0.05$ compared to LPS+hypoxia; Figure 3A), indicating that NADPH oxidase is required for the induction, but not the maintenance, of LPS+hypoxia LTD. Furthermore, we also applied apocynin onto hippocampal slices of WT mice. As shown in Figure 3B, apocynin completely blocked the LPS+hypoxia-induced LTD, leading to a recovery 95.8% ± 1.4% of baseline ($n = 5$, $p < 0.001$ compared to LPS+hypoxia in WT mice, $p > 0.05$ compared to LPS+hypoxia in CR3 KO mice).

To further confirm the involvement of NADPH oxidase, we tested a widely used NADPH oxidase-blocking peptide TAT-Phox (RKKRRQRRR-CSTRIRRQL) (Rey et al., 2001) and found that when included in the preincubation (for 1 hr) and perfusion

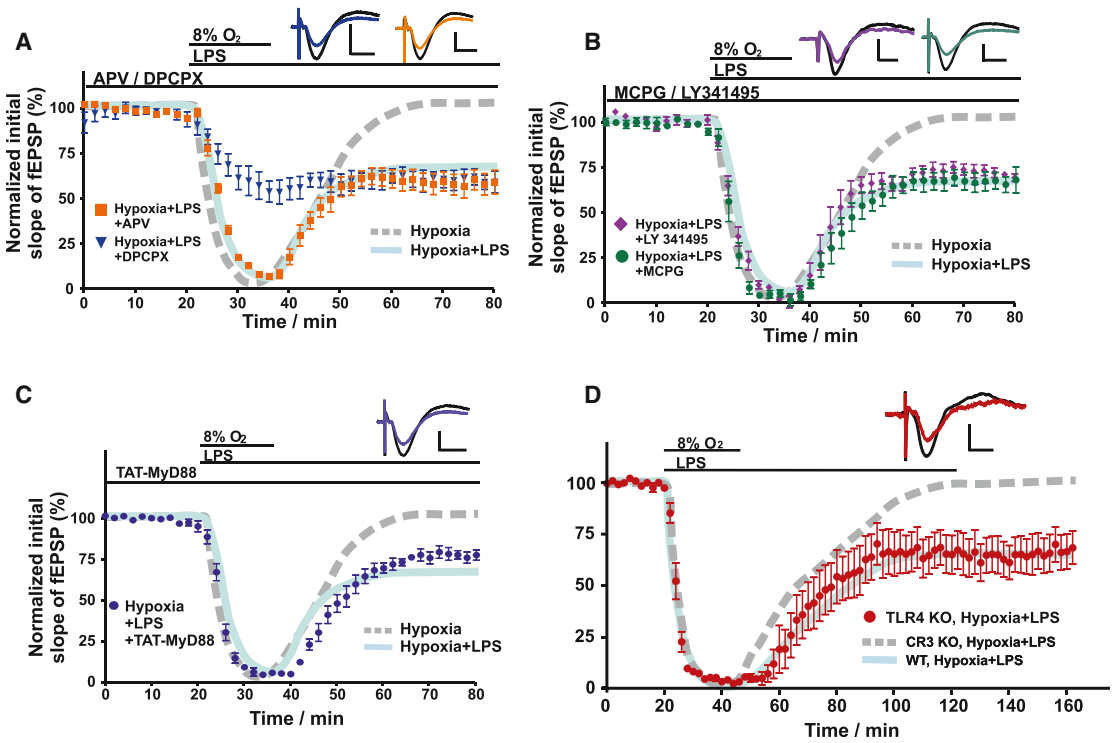

Figure 2. LPS+Hypoxia LTD Is Independent on NMDAR, mGluR, and TLR4

(A) APV (100 μM) or DPCPX (500 nM) was bath applied at least 20 min before the application of LPS+hypoxia and was included in all solutions throughout the experiment. Neither blocker significantly altered the LPS+hypoxia LTD. In (A)–(C), the dashed gray line indicates the hypoxia-only experiment in Figure 1A, while the solid blue line indicates hypoxia+LPS in Figure 1A.

(B) MCPG (250 μM) or LY341495 (100 μM) was applied the same way as blockers in (A). Neither blocker altered LPS+hypoxia LTD.

(C) TAT-MyD88 (1 μM) did not affect LPS+hypoxia LTD.

(D) LPS+hypoxia induced LTD in TLR4 KO mice. The dashed gray line indicates the LPS+hypoxia experiment in CR3 KO mice (from Figure 1E), while the solid blue line indicates hypoxia+LPS in WT mice (from Figure 1E). All error bars represent SEM.

solutions, TAT-Phox (1 μM) blocked LPS+hypoxia LTD in rat hippocampal slices (95.5% ± 1.1% of baseline 40 min after reperfusion, n = 6, $p < 0.01$ compared to LPS+hypoxia, and $p > 0.05$ compared to hypoxia alone; Figure 3C). The control scrambled peptide TAT-Phox^{scr} (RKKRRQRRR-CLRITRQSR) (1 μM) did not alter the level of LPS+hypoxia LTD (67.1% ± 10.5% of baseline, n = 4, $p > 0.05$ compared to LPS+hypoxia LTD without peptide; Figure 3C).

The pharmacological sensitivity of LPS+hypoxia LTD indicates that this is a form of LTD mediated by microglia activation and NADPH oxidase. Previous studies have shown that lower O_2 levels in some tissues enhance NADPH oxidase activity because increased glycolysis raises lactate/pyruvate ratios and thereby NADPH/NADP$^+$ ratios, which accelerate the production of superoxide from NADPH oxidase (Raddatz et al., 2011; Yang and Kahn, 2006). We postulated that lactic acid could be a contributing factor when released during hypoxia. Therefore, we tested whether lactic acid (3 mM) could mimic the actions of hypoxia to act synergistically with LPS to trigger LTD. We applied lactic acid, which decreased the pH of aCSF from 7.35 ± 0.01 to 7.01 ± 0.01 (n = 12). When the rat hippocampal slices were exposed to lactic acid alone for 30 min, basal transmission was not changed, remaining at 100.2% ± 1.2% of the baseline (n = 6; Figures 3D and 3E). However, when LPS was applied together with lactic acid, we observed a depression of synaptic transmission (79.5% ± 5.1% of baseline, n = 6, $p < 0.01$ compared to lactic acid only), which was completely blocked by apocynin (101.7% ± 4.9% of baseline, n = 6, $p < 0.01$ compared to LPS+lactic acid, and $p > 0.05$ compared to lactic acid only; Figures 3D and 3E). Statistics were based on fEPSPs 10 min after treatment when the depression was fully developed and stable. These data suggest that when NADPH oxidase is activated by an inflammatory stimulus (LPS in this experiment), lactic acid further enhances the activity of this enzyme to a degree that is sufficient to induce LTD.

Reactive Oxygen Species Produced by NADPH Oxidase Play a Key Role in the Induction of LPS+Hypoxia LTD

NADPH oxidase produces superoxide, a member of the reactive oxygen species (ROS) family, which generates other ROS such as hydrogen peroxide and peroxynitrite (Bedard and Krause, 2007). Increased ROS generation can potentially modulate synaptic transmission and is widely considered as a leading cause of neuronal dysfunction in neurodegenerative disorders (Gao et al., 2012; Reynolds et al., 2007). To test the role of ROS release in the induction of this form of LTD, we used ascorbic acid

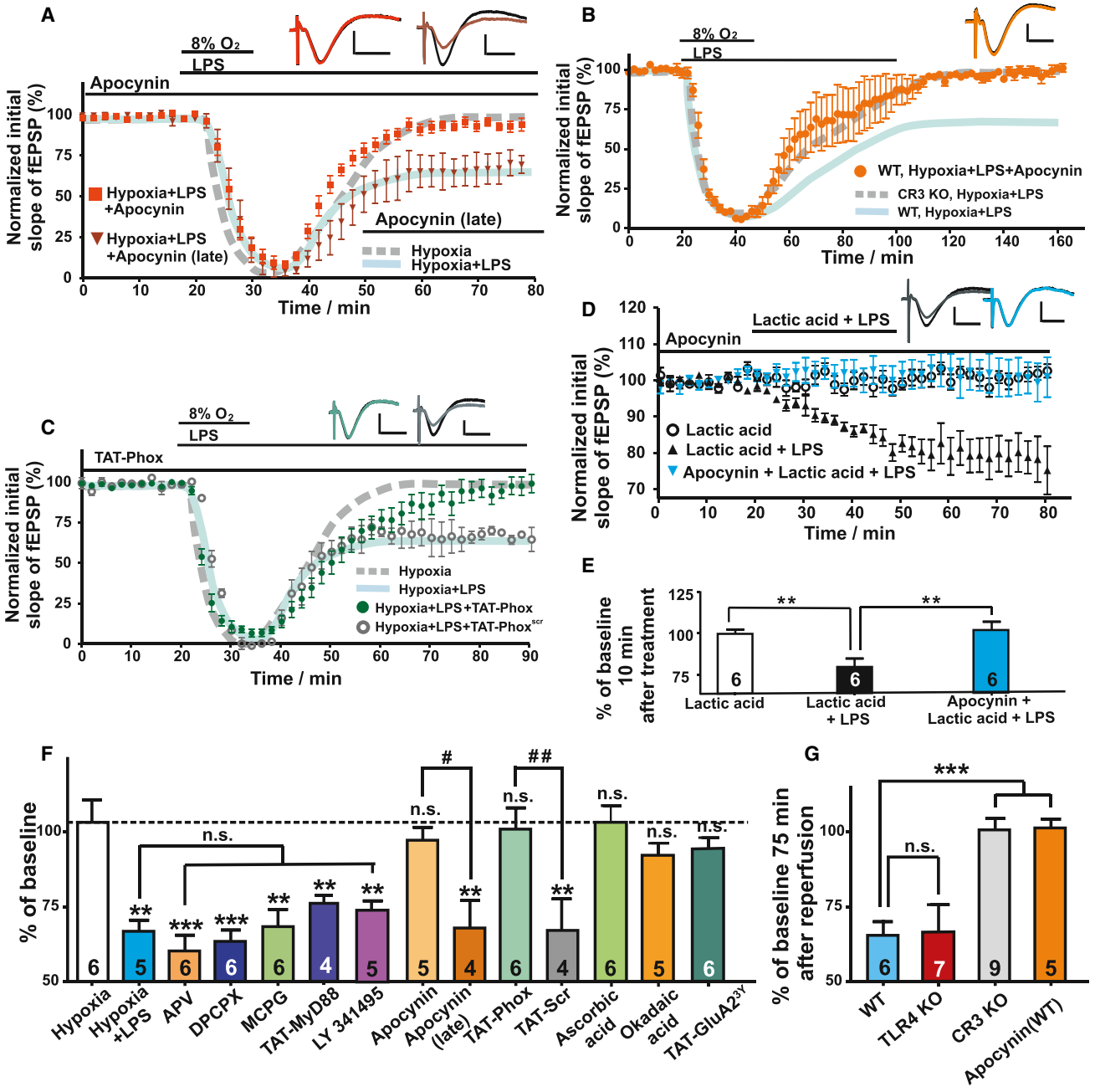

Figure 3. LPS+Hypoxia LTD Depends on Activation of NADPH Oxidase

(A) Apocynin (100 μM) was bath applied either at least 30 min before or 30 min after the application of LPS and hypoxia. Early application reversed LPS+hypoxia LTD, while late application did not have an effect. In (A) and (C), the dashed gray line indicates the hypoxia-only experiment (from Figure 1A), while the solid blue line indicates hypoxia+LPS (from Figure 1A).

(B) In slices of WT mice, apocynin was bath applied at least 30 min before and during treatment. The application of apocynin blocked the LPS+hypoxia LTD. The dashed gray line indicates the LPS+hypoxia experiment in CR3 KO mice (Figure 1E), while the solid blue line indicates hypoxia+LPS in WT mice (Figure 1E).

(C) NADPH oxidase-blocking peptide TAT-Phox (1 μM) inhibited LPS+hypoxia LTD, while scrambled peptide (TAT-Phox^{scr}, 1 μM) did not.

(D) Thirty minute application of lactic acid and LPS depressed basal transmission, while lactic acid alone did not alter it. Apocynin completely blocked this LPS+lactic acid-induced depression.

(E) Statistics of (D).

(F) Summary statistics of Figures 1A, 2A–2C, 3A, 3C, 4A, and 5B, and 5C. Statistics were based on fEPSPs 30 min after reperfusion except TAT-Phox and TAT-Scr, which were analyzed based on fEPSPs 40 min after reperfusion.

(G) Summary statistics of mice experiments, including Figures 1E, 2D, and 3B. Statistics were based on fEPSPs 75 min after reperfusion due to a slower recovery. All error bars represent SEM.

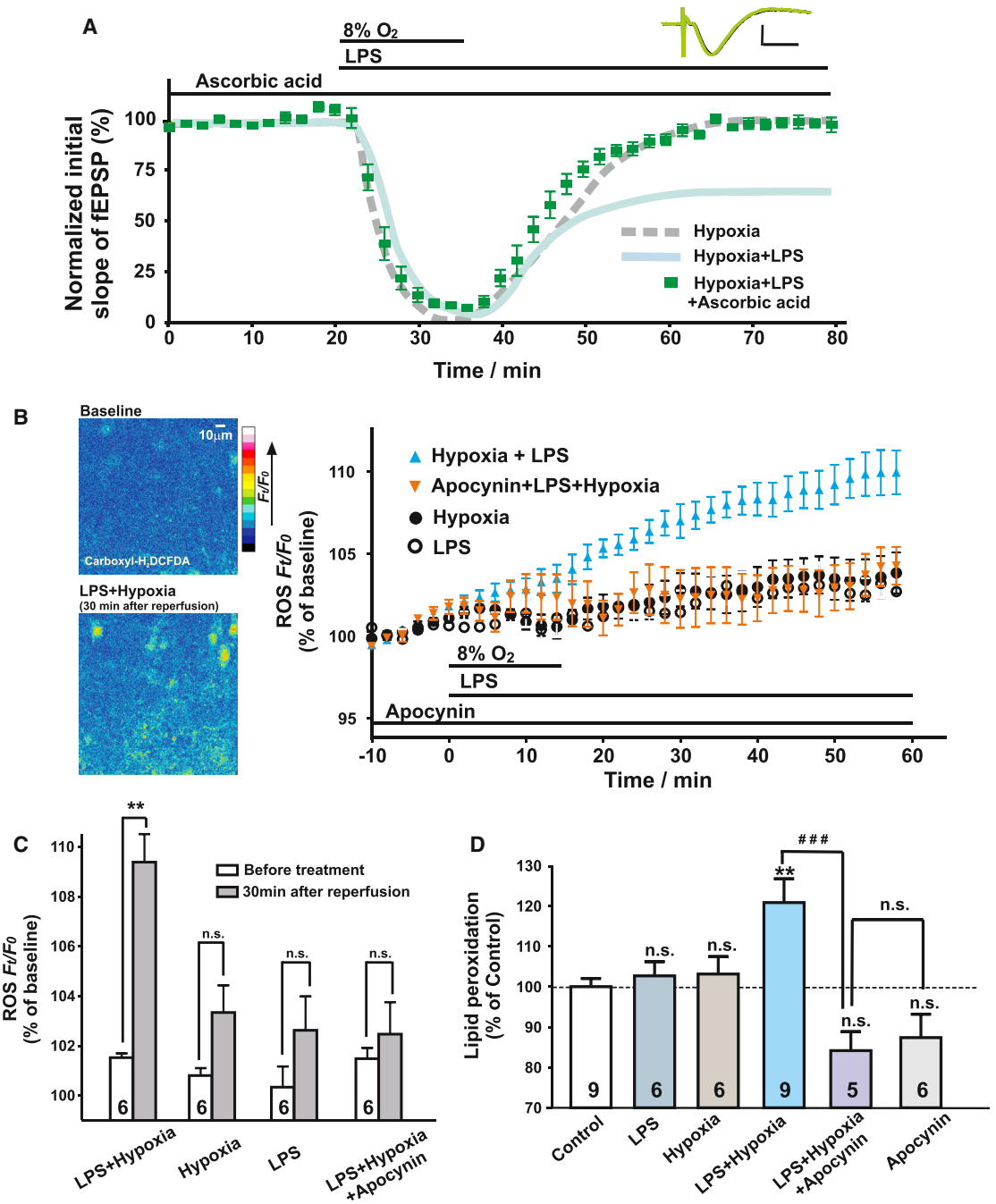

Figure 4. NADPH Oxidase-Produced Superoxide Plays a Key Role in the Induction of LPS+Hypoxia LTD

(A) Application of ascorbic acid (400 μM) blocked LPS+hypoxia LTD. The dashed gray line indicates the hypoxia-only experiment (from Figure 1A) while the solid blue line indicates hypoxia+LPS (from Figure 1A).

(B and C) LPS and hypoxia together caused a gradual increase of ROS fluorescent signal in the CA1 region but did not change fluorescence when applied separately (B). Apocynin blocked the LPS+hypoxia-induced ROS increase (statistics shown in C).

(D) LPS+hypoxia increased lipid peroxidation levels in slices, while separate applications had no effect. Apocynin completely blocked this increase. All error bars represent SEM.

(400 μM), a ROS scavenger, in the preincubation solution (for 1 hr) and recording solution. As shown in Figure 4A, ascorbic acid completely blocked LPS+hypoxia LTD in rat hippocampal slices (102.4% ± 5.9% of baseline, n = 6, $p < 0.01$ compared to LPS+hypoxia, and $p > 0.05$ compared to hypoxia alone). This result, combined with the data using NADPH oxidase

inhibitors (Figures 3A and 3B), suggests that LPS+hypoxia LTD is induced by ROS release through activation of NADPH oxidase.

To provide two independent indications that LPS and hypoxia synergistically induced ROS generation in rat hippocampal slices, first we detected ROS changes by two-photon imaging of a ROS-sensitive dye 5-(and-6)-carboxy-2′,7′-dichlorodihydrofluorescein diacetate (Carboxy-H_2DCFDA) (Fekete et al., 2008) and, second, we measured lipid peroxidation levels in treated brain slices. The nonfluorescent carboxy-H_2DCFDA is converted to a green fluorescent form when it is oxidized by the activity of ROS, and the generation of ROS is indicated by the progressive accumulation of green fluorescence within cells (Halliwell and Whiteman, 2004). As shown in Figures 4B and 4C, the fluorescence in the stratum radiatum layer of CA1 did not significantly increase when slices were exposed to either hypoxia or LPS separately, although there was a nonsignificant upward trend possibly due to tissue illumination (hypoxia: 103.3% ± 1.1% of baseline, $n = 6$, $p > 0.05$ compared to a preapplication control period; LPS: 102.6% ± 1.4% of baseline, $n = 6$, $p > 0.05$ compared to a preapplication control period). However, when both hypoxia and LPS were present, the average fluorescence intensity steadily increased to 109.6% ± 1.4% of baseline ($n = 6$, $p < 0.01$ compared to baseline) at 30 min after reperfusion of normoxic solution, indicating a significant increase in ROS levels upon LPS+hypoxia treatment. This increase of ROS fluorescent signal was completely blocked by the NADPH oxidase inhibitor apocynin (102.5% ± 1.3% of baseline, $n = 6$; Figures 4B and 4C; $p > 0.05$ compared to baseline).

We further confirmed that LPS and hypoxia cause oxidative stress in slices by measuring lipid peroxidation levels 30 min after reperfusion in slices treated identically as in the electrophysiology experiments. As shown in Figure 4D, LPS and hypoxia together increased lipid peroxidation to 120.8% ± 5.9% of control level ($n = 9$, $p < 0.01$ compared to control), whereas when applied separately, neither LPS nor hypoxia increased lipid peroxidation level (102.7% ± 3.6% and 103.1% ± 4.3% of control respectively, $n = 6$ each, $p > 0.05$ compared to control). Apocynin treatment nonsignificantly decreased the baseline (87.4% ± 5.8% of control, $n = 5$, $p > 0.05$ compared to control) and completely blocked the LPS-hypoxia-induced increase of lipid peroxidation in slices (combination of LPS, hypoxia, and apocynin was 84.2% ± 4.7% of control, $n = 6$, $p > 0.05$ compared to apocynin alone, and $p < 0.001$ compared to LPS+hypoxia without apocynin). Therefore, both imaging Carboxy-H_2DCFDA fluorescence and measuring lipid peroxidation indicated that ROS generation is significantly increased in brain slices when both LPS and hypoxia are applied together but not separately.

To test whether lipid peroxidation leads to acute cell damage during the time course of these experiments, we measured lactate dehydrogenase (LDH) release as an indicator of acute cell death. As shown in Figure S3A, LPS+hypoxia did not increase LDH release from rat hippocampal slices up to 3 hr after treatment. In addition, intracellular calcium ($[Ca^{2+}]_i$) in hippocampal neurons did not change significantly and there was no apparent loss of dye, which might occur if cells were damaged (Figures S3B–S3D). Furthermore, cells in slices showed no shrinkage or swelling throughout the whole experiment, indicating that the slices were still in a relatively healthy state.

PP2A Activation Plays an Important Role in LPS+Hypoxia LTD

After confirming the production of superoxide from NADPH oxidase after microglial CR3 activation, we further explored the mechanism in neurons that leads to LTD. Protein phosphatase 2A (PP2A) has been shown to play a key role in the induction and maintenance of LTD (Mulkey et al., 1993; Nicholls et al., 2008). Furthermore, previous studies have shown that superoxide and its product hydrogen peroxide can increase PP2A activity (Caraballo et al., 2011; Maalouf and Rho, 2008; Sheth et al., 2009). Therefore, we postulated that ROS-dependent activation of PP2A could contribute to LPS+hypoxia LTD.

To test this possibility, we measured PP2A activity in rat hippocampal slices 30 min after reperfusion of normoxic solution and found that PP2A activity was significantly increased by LPS+hypoxia treatment (143.6% ± 6.2% of control level, $n = 6$, $p < 0.001$ compared to control group) versus significantly smaller changes in LPS alone (119.9% ± 4.3%, $n = 6$, $p < 0.05$ compared to LPS+hypoxia) or hypoxia alone (118.5% ± 6.6%, $n = 6$, $p < 0.01$ compared to LPS+hypoxia) (Figure 5A).

Furthermore, we applied okadaic acid (250 nM), a PP2A blocker, in preincubation solution (for 1 hr) and found that LPS+hypoxia LTD was blocked (91.4% ± 4.0% of baseline, $n = 5$, $p < 0.05$ compared to LPS+hypoxia, and $p > 0.05$ compared to hypoxia alone; Figure 5B). Taken together, our results indicate an important role of PP2A activation in the induction of LPS+hypoxia LTD.

LPS+Hypoxia LTD Is Induced by GluA2-Mediated AMPAR Endocytosis

A-amino-3-hydroxy-5-methyl-4-isoxazolepropionic acid receptor (AMPAR) endocytosis is a well-known mechanism underlying NMDAR-dependent LTD in CA1 pyramidal neurons (Beattie et al., 2000). It has been shown that AMPAR endocytosis is dependent on the GluA2 subunit and this process can be blocked by a peptide ($GluA2^{3Y}$) that mimics the end of the GluA2 C terminus (Ahmadian et al., 2004).

We examined whether LPS+hypoxia LTD was mediated by GluA2-dependent AMPAR endocytosis, by testing the sensitivity to the $GluA2^{3Y}$-interfering peptide. Using extracellular field potential recordings, we found that when 1 μM TAT-$GluA2^{3Y}$ (YGRKKRRQRRR-YKEGYNVYG) was included in the preincubation (for 1 hr) and perfusion solutions, the induction of LPS+hypoxia LTD was blocked in rat hippocampal slices (fEPSPs were 92.2% ± 3.9% of baseline, $n = 6$, $p < 0.01$ compared to LPS+hypoxia, and $p > 0.05$ compared to hypoxia alone; Figure 5C), suggesting a key role of AMPAR endocytosis in LPS+hypoxia LTD.

We next investigated whether the release of superoxide from exogenous sources within brain slices would generate LTD that is similar to LPS+hypoxia LTD and whether this LTD would be sensitive to TAT-$GluA2^{3Y}$. To address this question, we used xanthine/xanthine oxidase (X/XO), a widely used superoxide-generating system (Knapp and Klann, 2002), to see whether this would mimic the effect of LPS+hypoxia. As shown in Figures 5D and 5E, we applied X/XO (20 μg/ml/25 μg/ml) onto the slices for 20 min and observed a transient depression of synaptic transmission. After reperfusion with normal aCSF,

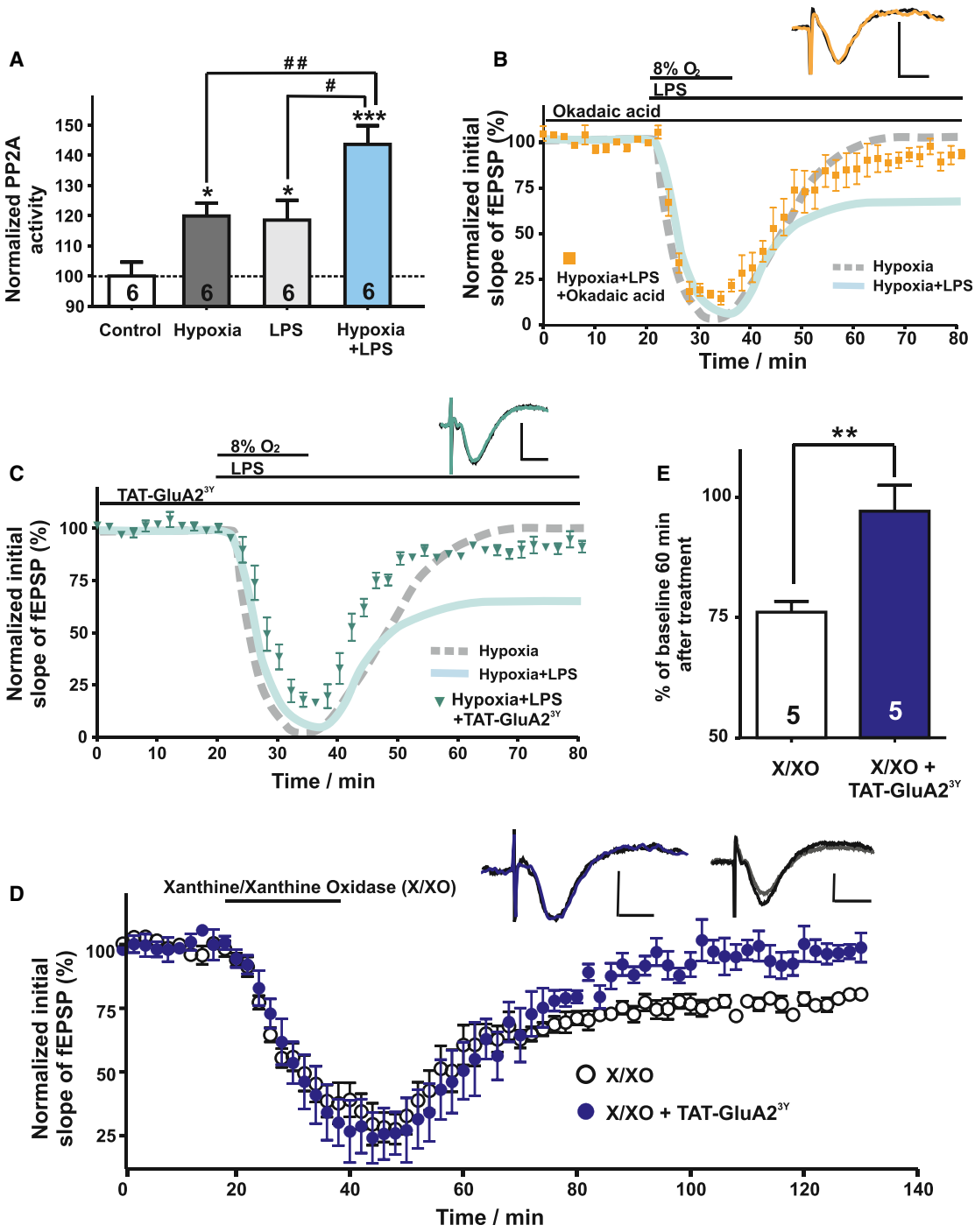

Figure 5. LPS+Hypoxia LTD Is Induced by PP2A Activation and GluA2-Mediated AMPAR Endocytosis

(A) PP2A activity assay showed that PP2A activity was significantly increased by LPS+hypoxia treatment versus significantly smaller increases in LPS or hypoxia alone.

(B) Slices were preincubated in okadaic acid (250 nM) for 1 hr before experiments. Okadaic acid blocked the induction of LPS+hypoxia LTD. In (B) and (C), the dashed gray line indicates the hypoxia-only experiment (from Figure 1A), while the solid blue line indicates hypoxia+LPS (from Figure 1A).

(C) TAT-GluA2^{3Y} (1 μM) blocked the induction of LPS+hypoxia LTD.

(D) Twenty minute perfusion of X (20 μg/ml)/XO (25 μg/ml) induced an LTD, which was blocked by TAT-GluA2^{3Y} (1 μM, 1 hr preincubation and present all through the experiments).

(E) Statistics of (D) 60 min after treatment. All error bars represent SEM.

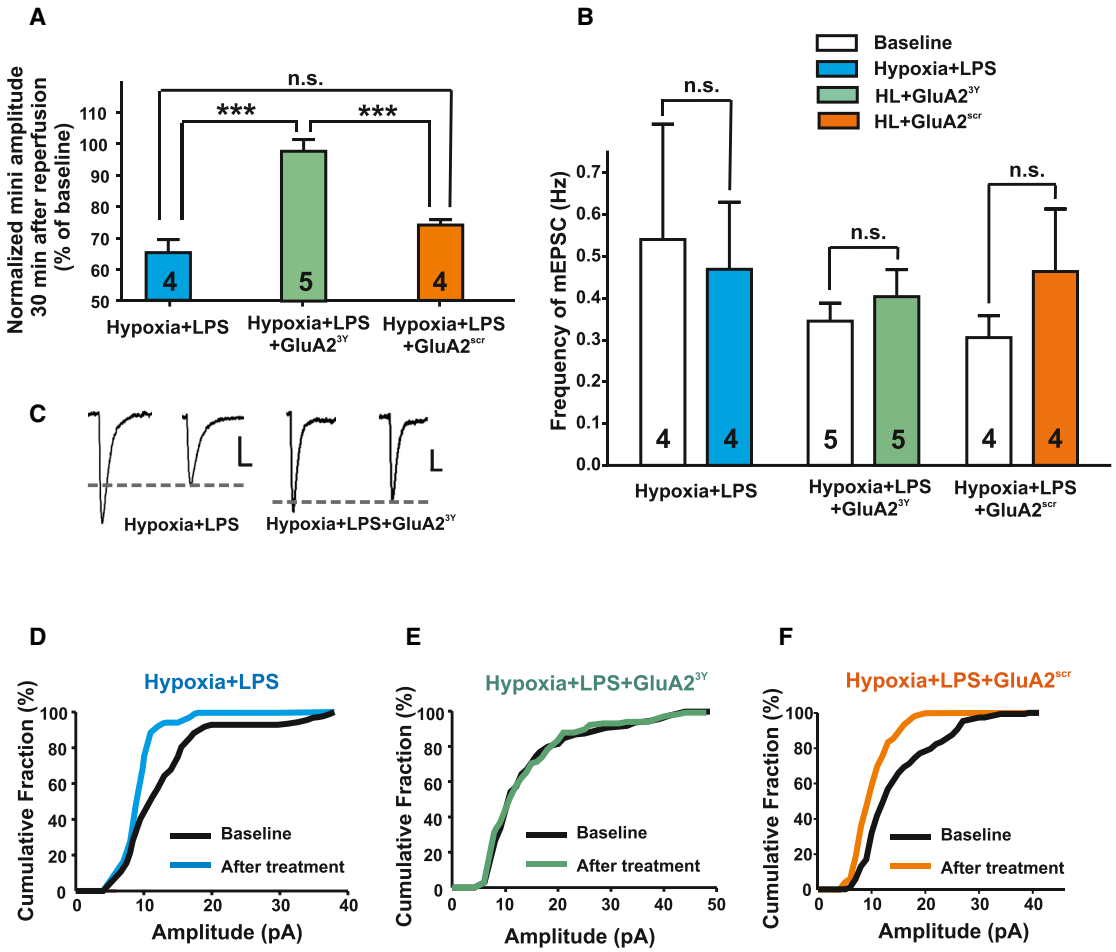

Figure 6. LPS+Hypoxia LTD Is Mediated by Postsynaptic Mechanism Involving GluA2-Mediated AMPAR Endocytosis

(A) LPS and hypoxia caused a decrease of mEPSC amplitude in CA1 neurons. This amplitude decrease was blocked by GluA2^{3Y} peptide but not by a scrambled control GluA2^{scr} (both peptides applied at 50 μg/ml in internal solution).

(B) Measurement of mEPSC frequency shows no significant difference between baseline and 30 min after reperfusion.

(C) Sample average traces of (A). Scale bars represent 5 ms (horizontal) and 5 pA (vertical).

(D–F) Cumulative fractions of mEPSC amplitude before and after LPS+hypoxia treatment in control (D), in GluA2^{3Y} (E), and in GluA2^{scr} (F). All error bars represent SEM.

synaptic transmission recovered to a decreased level (76.1% ± 2.2% of baseline 60 min after treatment, n = 5), further confirming an important role of ROS in the induction of LPS+hypoxia LTD. When included in preincubation (1 hr) and perfusion solutions, TAT-GluA2^{3Y} (1 μM) blocked X/XO-induced LTD, resulting in a full recovery 60 min after X/XO treatment (97.1% ± 5.4% of baseline, n = 5, $p < 0.01$ compared to X/XO; Figures 5D and 5E).

To further investigate the role for AMPAR internalization in LPS+hypoxia LTD, we performed whole-cell voltage-clamp recordings of miniature excitatory postsynaptic currents (mEPSCs) in CA1 pyramidal neurons with GluA2^{3Y} (YKEGYNVYG) or the scrambled peptide GluA2^{scr} (AKEGANVAG) in the recording pipette. After obtaining a stable baseline (10 min), we applied hypoxic aCSF (8% O_2 saturated) with LPS (10 μg/ml) for 15 min, followed by reperfusion of normoxic aCSF containing LPS. As shown in Figures 6A, 6C, and 6D, the treatment of LPS and hypoxia resulted in a decrease of mEPSC amplitude (65.1% ± 4.2% of baseline, n = 4, $p < 0.001$ compared to baseline) 20–25 min after reperfusion. When GluA2^{3Y} (50 μg/ml) was included in the recording pipette, LPS+hypoxia LTD was blocked (mEPSC amplitude 97.4% ± 3.7% of baseline, n = 5, $p < 0.001$ compared to LPS+hypoxia; Figures 6A, 6C, and 6E), while inclusion of GluA2^{scr} did not change the level of LPS+hypoxia LTD (73.8% ± 1.7% of baseline, n = 4, $p > 0.05$ compared to LPS+hypoxia; Figures 6A and 6F). As shown in Figure 6B, the treatments did not change mEPSC frequency. Taken together, our results indicate a key role for AMPAR endocytosis in the expression of LPS+hypoxia LTD.

As AMPAR endocytosis has been known to play an important role in LTD that is induced by other stimuli (Beattie et al., 2000; Collingridge et al., 2010), we further tested whether the LPS+hypoxia LTD that we observed would occlude subsequent LTD triggered by other methods. As shown in Figure S4, LPS+hypoxia LTD did not occlude low-frequency stimulation (LFS)-induced

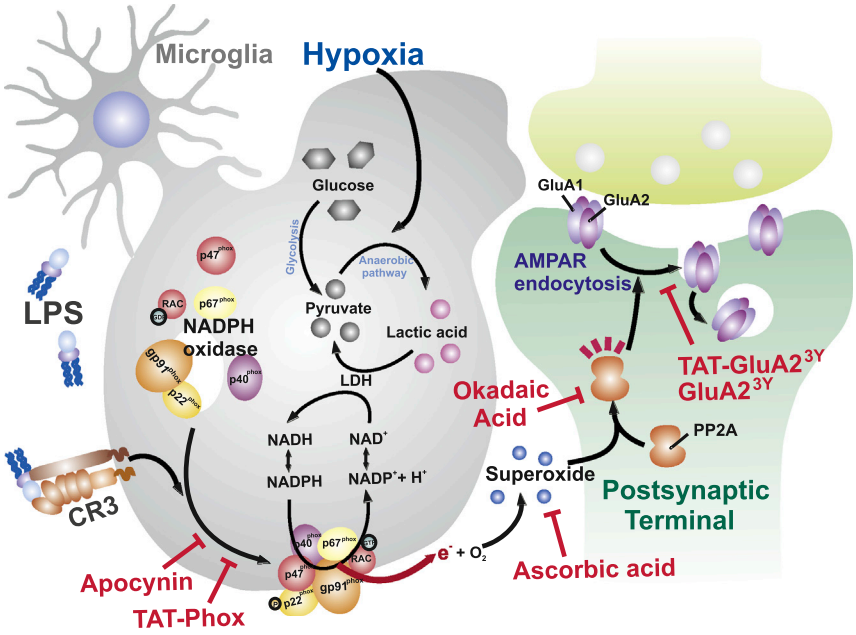

Figure 7. Summary Figure
Inflammatory stimulus LPS and hypoxia synergistically activate NADPH oxidase in a CR3-dependent manner. NADPH oxidase produces superoxide, which then activates PP2A and induces LTD via AMPAR internalization in postsynaptic terminals.

LTD (NMDAR dependent) or dihydroxyphenylglycine (DHPG)-induced LTD (mGluR dependent).

DISCUSSION

Our results indicate that stimulation of microglial CR3 can trigger LTD in surrounding neurons. The experiments using the A1 receptor antagonist (Figure 2A) revealed that this surprising communication between microglia and neurons can occur within 15 min after applying the inflammatory stimulus LPS in combination with transient hypoxia. Although LPS also acts through other receptor systems such as TLR4 in addition to CR3 (Kettenmann et al., 2011), our results showing the inability of LPS and hypoxia to elicit LTD in the CR3 KO mice demonstrate a critical role of microglial CR3 in regulating synaptic plasticity. TLR4 does not appear to be an essential receptor in this process as LPS+hypoxia LTD was still observed in TLR4 KO mice, and a peptide that disrupts TLR4-MyD88 interactions and LPS-triggered cytokine formation (Hines et al., 2013) did not impair LPS+hypoxia LTD. Microglial CR3-triggered LTD results from NADPH oxidase activation and is independent of NMDAR or mGluR stimulation or a specific pattern of synaptic activation. The production of superoxide from NADPH oxidase induces LTD via activation of PP2A and GluA2-mediated AMPAR internalization (Figure 7). Our study identifies a form of relatively rapid microglia-neuronal communication through which an enhanced neuroinflammatory response in microglia directly modulates synaptic transmission. These results provide a paradigm by which microglial NADPH oxidase can modify neuronal activity and synaptic function.

CR3 has recently been shown to have important roles in the physical removal of synapses during development in a process called synaptic pruning (Schafer et al., 2012; Stephan et al., 2012; Stevens et al., 2007). Our findings indicate that there is also a role for microglial CR3 in modifying the dynamic properties of active synapses by triggering a reduction in synaptic efficacy. Given a known correlation between spine structure and synaptic strength (Kasai et al., 2010), the link between CR3 activation and synaptic depression could be relevant to the microglia-induced synaptic pruning. The depression of synaptic efficacy could be a prelude to the direct involvement of microglia in synaptic pruning, which has a longer time of onset than LTD.

The activation of PP2A has been recognized as a key step in induction of stimulus-dependent and chemical-dependent LTD (Mulkey et al., 1993; Nicholls et al., 2008), and there are several possible mechanisms leading from LTD-inducing synaptic activation to PP2A activation (Pi and Lisman, 2008). Although the LPS+hypoxia LTD that we describe here occurs independently of synaptic activation, we explored the potential involvement of PP2A as studies in both neurons and other cell types have demonstrated a link between ROS generation and PP2A activation (Caraballo et al., 2011; Maalouf and Rho, 2008; Sheth et al., 2009). We found that LPS+hypoxia induction of LTD was associated with the activation of PP2A and was blocked by okadaic acid, an inhibitor of PP2A, suggesting that the ROS generation by NADPH oxidase in microglia could cause PP2A activation in neurons leading to AMPAR internalization.

NADPH oxidase has been shown to be a key enzyme that mediates neurotoxicity in trauma, stroke, and various neurodegenerative disorders including Alzheimer's disease and Parkinson's disease (Block et al., 2007; Gao et al., 2012). Oxidative stress has been implicated in numerous studies of neurodegeneration, and various methods to attenuate oxidative stress have shown promising results in clinical studies (Barnham et al., 2004), suggesting that targeting the source of the oxidative stress signals such as NADPH oxidase may be useful in alleviating some of the deterioration in neurodegeneration (Drummond et al., 2011; Gao et al., 2012). The activation of NADPH oxidase, shown by our study to reduce synaptic efficiency, may contribute to the memory impairments and synaptic disruptions that are characteristics of dementias and may be a therapeutic target to alleviate memory loss in these brain disorders.

Decreased cerebral blood flow (CBF) (possibly triggered by ministroke infarcts or impaired neurovascular coupling) is considered to be a major contributing factor to cognitive impairment and is recognized as an important risk factor for dementia (Zlokovic, 2011). Hypoxia associated with reduced CBF can enhance damage caused by neuroinflammation (Peers et al., 2009; Zlokovic, 2011). Containment of neuroinflammation is

important for reducing cognitive decline and it has been suggested that unrestrained neuroinflammation may lead to increased predisposition to Alzheimer's disease (Jonsson et al., 2013). Our finding that hypoxia enhances the impact of LPS on synaptic function suggests the importance of preventing CNS hypoxia for restraining the effects of neuroinflammation in vivo. Further studies on the impact of microglial CR3-mediated LTD will be important in determining the degree to which it contributes to the memory impairments and synaptic disruptions that are characteristics of dementias and whether it could be a therapeutic target to alleviate memory loss before there is cell loss.

EXPERIMENTAL PROCEDURES

Animals

Sprague-Dawley rats (postnatal days 18 to 23) were used in most of the experiments unless otherwise indicated. CR3 KO mice (1–3 months old), TLR4 KO mice (1–3 months old), and WT controls (1–3 months old) were purchased from Jax Mice.

Hippocampal Slice Preparation

Animals were anesthetized and decapitated according to protocols approved by the University of British Columbia committee on animal care. Transverse hippocampal slices were prepared in ice-cold slicing solution followed by 1 hr recovery at room temperature.

Field Recording

Field recordings were performed in the Schaffer collateral pathway in CA1 region at room temperature (22°C–25°C). fEPSP signals were amplified with an AC amplifier (Molecular Devices), digitized using a Digidata 1440A interface board (Axon Instruments), and transferred to a computer with Clampex 10.0 (Molecular Devices). fEPSPs were quantified by initial slope, which in further analysis was normalized to the mean of baseline. The mean normalized fEPSP slope was plotted as a function of time with every dot representing the average of four sweeps (2 min) and error bars representing SEM. Statistics were based on mean values of eight sweeps within 4 min around the chosen time point.

In the experiments on brain slices from rats, LTD was induced by hypoxic stimulus (8% O_2, 5% CO_2, 87% N_2 saturated aCSF for 15 min) with 10 μg/ml LPS and data were included when recordings were stable by 40 min after reperfusion. LTD was induced by hypoxic stimulus (8% O_2-saturated aCSF for 25 min) with 15 μg/ml LPS in the experiments on brain slices from mice and data were included when recordings were stable by 75 min after reperfusion. It required higher LPS concentration and longer hypoxia exposure to trigger LTD in mice (1–3 months old) than in rats (18–23 days). This change may be due to differences in the sensitivity to LPS and/or hypoxia between mice and rats at these different ages.

Field recording experiments were not performed in a blinded manner. The experiments in mice were performed in a randomized manner, while experiments in rats were not.

Whole-Cell Recording

Whole-cell recordings were performed at room temperature on CA1 pyramidal neurons that were voltage clamped at −70 mV. mEPSC signals were amplified using a Multiclamp 700B amplifier (Axon Instruments), digitized using a 1440A digidata, and recorded with Clampex 10.0. Data were analyzed using MiniAnalysis (Synaptosoft).

Two-Photon Imaging

ROS were monitored by Carboxyl-H_2DCFDA, while $[Ca^{2+}]_i$ was indicated by Rhod-2 AM. We successfully stained neurons with Rhod-2 (in contrast to the typical astrocyte staining) when we used a previously published protocol that was demonstrated to facilitate loading of –AM dyes into neurons in brain slices (Trevelyan et al., 2006) and included cremophor in the staining procedure as described in the Supplemental Experimental Procedures. Imaging was performed with a two-photon laser-scanning microscope (Zeiss LSM510-Axioskop-2) directly coupled to a Mira Ti:sapphire laser (~100 fs pulses, 76 MHz, Coherent). Images were obtained at 40–50 μm below the surface and were analyzed after experiments using ImageJ. Fluorescent signals were quantified as F_t/F_0, where F_t and F_0 represent fluorescence signal at a given time during treatments and that of the baseline, respectively.

Lipid Peroxidation Assay

Lipid peroxidation assay kit (Biomedical Research Service Center, State University of New York at Buffalo) was used to assess oxidative stress in slices. Results were normalized by total protein levels of the samples.

LDH Assay

Extracellular LDH was measured using LDH assay kits (State University of New York at Buffalo). aCSF with 5% Triton X-100, a detergent to break cell membranes, was used as the positive control. Cell death was calculated as percentage of superfusate LDH compared to the sum of superfusate LDH and brain slice LDH.

Western Blotting

The brain slices were homogenized using lysis buffer. The homogenates were then centrifuged at 13,000 × *g* (20 min, 4°C) and prepared as samples according to protein concentrations. After SDS/PAGE, proteins were transferred to PVDF membranes. Mouse anti-CD11b monoclonal antibody (Abcam, 1:500 [2 μg/ml]) and anti-mouse secondary antibody (1:2,000) conjugated to horseradish peroxidase were used. Bands were visualized using enhanced chemiluminescence (ECL; Amersham Bioscience).

Immunohistochemistry

For Figure 1C and Figure S2A, wild-type and CD11b knockout mice were perfused intracardially with paraformaldehyde (PFA). Brains were postfixed in PFA and cryosectioned (40 μm) as free-floating coronal slices. Sections were incubated with blocking solution, followed by primary antibodies directed against Iba-1 (1:1,000 [0.5 μg/ml]; Wako) and CD11b (1:500 [2 μg/ml]; AbD Serotec) and secondary antibodies (Alexa-Fluor-488-conjugated goat anti-rabbit IgG and Alexa-Fluor-546-conjugated goat anti-rat IgG, 1:500 [4 μg/ml]; Molecular Probes).

For Figure S2B, hippocampal slices were prepared as previously described, then fixed by PFA. Immunohistochemistry was performed on fixed tissue from CR3 KO mice to label CD11b and Iba-1 epitopes. The tissue was incubated with antibodies against CD11b or Iba-1 and washed before incubation with either Alexa-594-conjugated anti-rat IgG (4 μg/ml) or Alexa-488-conjugated anti-rabbit IgG (4 μg/ml) antibodies, respectively.

PP2A Activity Assay

PP2A Immunoprecipitation Phosphatase Assay Kits (Millipore) were used to assess PP2A activity in slices. PP2A activity was measured by reaction with phosphopeptide. Results were normalized by total protein level of the samples.

Peptide Design

The blocking peptide of NADPH oxidase was designed to interfere with the assembly of NADPH oxidase components (Rey et al., 2001). The TAT sequence was attached to transport functional peptides through the plasma membrane (Mann and Frankel, 1991; Schwarze et al., 2000). Peptides were generated by Anaspec, and the sequences are as follows: TAT-Phox: RKKRRQRRR-CSTRIRRQL; TAT-Phox^{scr}: RKKRRQRRR-CLRITRQSR.

The blocking peptide TAT-MyD88 mimics the BB-loop of MyD88 TIR domains and was designed to interfere with the interaction between toll-like receptor 4 (TLR4) and myeloid differentiation primary response gene 88 (MyD88) (Hines et al., 2013; Loiarro et al., 2005). Peptides were generated by Anaspec, and the sequence is as follows: TAT-MyD88: YGRKKRRQRRR-RDVLPGT.

The blocking peptides of GluA2-mediated AMPAR endocytosis were designed to mimic the end of the GluA2 C terminus and interfere with AMPAR endocytosis (Ahmadian et al., 2004). Peptides were generous gifts

from Dr. Yu Tian Wang's lab. The sequences were as follows: TAT-GluA2^{3Y}: YGRKKRRQRRR-YKEGYNVYG; GluA2^{3Y}: YKEGYNVYG; GluA2^{scr}: AKEGANVAG.

Data Analysis and Statistics

All values shown in the figures are the mean ± SEM with baselines or controls set as 100%. n is the number of experiments conducted. One hippocampal slice was used for one experiment, unless otherwise indicated. Statistical significance was assessed using one-way ANOVA (* or #: $p < 0.05$; ** or ##: $p < 0.01$; *** or ###: $p < 0.001$).

SUPPLEMENTAL INFORMATION

Supplemental Information includes Supplemental Experimental Procedures and four figures and can be found with this article online at http://dx.doi.org/10.1016/j.neuron.2014.01.043.

ACKNOWLEDGMENTS

This work was supported by operating grants from the Canadian Institutes of Health Research (CIHR Funding reference numbers 8545 and 10677) (B.A.M.), a Canada Research Chair (B.A.M.), a Natural Sciences and Engineering Research Council of Canada Studentship Award (A.M.), a CIHR studentship award (R.W.Y.K.), and a Heart and Stroke Studentship Award (L.D.O.). We thank Dr. Yu Tian Wang, Dr. Terry Snutch, and Dr. Tony Phillips for comments on the manuscript and Dr. Wang for the generous gift of 3Y peptides.

Accepted: January 15, 2014
Published: March 13, 2014

REFERENCES

Ahmadian, G., Ju, W., Liu, L., Wyszynski, M., Lee, S.H., Dunah, A.W., Taghibiglou, C., Wang, Y., Lu, J., Wong, T.P., et al. (2004). Tyrosine phosphorylation of GluR2 is required for insulin-stimulated AMPA receptor endocytosis and LTD. EMBO J. *23*, 1040–1050.

Barnham, K.J., Masters, C.L., and Bush, A.I. (2004). Neurodegenerative diseases and oxidative stress. Nat. Rev. Drug Discov. *3*, 205–214.

Beattie, E.C., Carroll, R.C., Yu, X., Morishita, W., Yasuda, H., von Zastrow, M., and Malenka, R.C. (2000). Regulation of AMPA receptor endocytosis by a signaling mechanism shared with LTD. Nat. Neurosci. *3*, 1291–1300.

Bedard, K., and Krause, K.H. (2007). The NOX family of ROS-generating NADPH oxidases: physiology and pathophysiology. Physiol. Rev. *87*, 245–313.

Block, M.L., Zecca, L., and Hong, J.S. (2007). Microglia-mediated neurotoxicity: uncovering the molecular mechanisms. Nat. Rev. Neurosci. *8*, 57–69.

Caraballo, J.C., Yshii, C., Butti, M.L., Westphal, W., Borcherding, J.A., Allamargot, C., and Comellas, A.P. (2011). Hypoxia increases transepithelial electrical conductance and reduces occludin at the plasma membrane in alveolar epithelial cells via PKC-ζ and PP2A pathway. Am. J. Physiol. Lung Cell. Mol. Physiol. *300*, L569–L578.

Collingridge, G.L., Peineau, S., Howland, J.G., and Wang, Y.T. (2010). Long-term depression in the CNS. Nat. Rev. Neurosci. *11*, 459–473.

Drummond, G.R., Selemidis, S., Griendling, K.K., and Sobey, C.G. (2011). Combating oxidative stress in vascular disease: NADPH oxidases as therapeutic targets. Nat. Rev. Drug Discov. *10*, 453–471.

Dunwiddie, T.V., and Masino, S.A. (2001). The role and regulation of adenosine in the central nervous system. Annu. Rev. Neurosci. *24*, 31–55.

Fekete, A., Vizi, E.S., Kovács, K.J., Lendvai, B., and Zelles, T. (2008). Layer-specific differences in reactive oxygen species levels after oxygen-glucose deprivation in acute hippocampal slices. Free Radic. Biol. Med. *44*, 1010–1022.

Flaherty, S.F., Golenbock, D.T., Milham, F.H., and Ingalls, R.R. (1997). CD11/CD18 leukocyte integrins: new signaling receptors for bacterial endotoxin. J. Surg. Res. *73*, 85–89.

Gao, H.M., Zhou, H., Zhang, F., Wilson, B.C., Kam, W., and Hong, J.S. (2011). HMGB1 acts on microglia Mac1 to mediate chronic neuroinflammation that drives progressive neurodegeneration. J. Neurosci. *31*, 1081–1092.

Gao, H.M., Zhou, H., and Hong, J.S. (2012). NADPH oxidases: novel therapeutic targets for neurodegenerative diseases. Trends Pharmacol. Sci. *33*, 295–303.

Halliwell, B., and Whiteman, M. (2004). Measuring reactive species and oxidative damage in vivo and in cell culture: how should you do it and what do the results mean? Br. J. Pharmacol. *142*, 231–255.

Hanisch, U.K., and Kettenmann, H. (2007). Microglia: active sensor and versatile effector cells in the normal and pathologic brain. Nat. Neurosci. *10*, 1387–1394.

Hauss-Wegrzyniak, B., Lynch, M.A., Vraniak, P.D., and Wenk, G.L. (2002). Chronic brain inflammation results in cell loss in the entorhinal cortex and impaired LTP in perforant path-granule cell synapses. Exp. Neurol. *176*, 336–341.

Hickman, S.E., Kingery, N.D., Ohsumi, T.K., Borowsky, M.L., Wang, L.C., Means, T.K., and El Khoury, J. (2013). The microglial sensome revealed by direct RNA sequencing. Nat. Neurosci. *16*, 1896–1905.

Hines, D.J., Choi, H.B., Hines, R.M., Phillips, A.G., and MacVicar, B.A. (2013). Prevention of LPS-induced microglia activation, cytokine production and sickness behavior with TLR4 receptor interfering peptides. PLoS ONE *8*, e60388.

Jonsson, T., Stefansson, H., Steinberg, S., Jonsdottir, I., Jonsson, P.V., Snaedal, J., Bjornsson, S., Huttenlocher, J., Levey, A.I., Lah, J.J., et al. (2013). Variant of TREM2 associated with the risk of Alzheimer's disease. N. Engl. J. Med. *368*, 107–116.

Kasai, H., Fukuda, M., Watanabe, S., Hayashi-Takagi, A., and Noguchi, J. (2010). Structural dynamics of dendritic spines in memory and cognition. Trends Neurosci. *33*, 121–129.

Kettenmann, H., Hanisch, U.K., Noda, M., and Verkhratsky, A. (2011). Physiology of microglia. Physiol. Rev. *91*, 461–553.

Kettenmann, H., Kirchhoff, F., and Verkhratsky, A. (2013). Microglia: new roles for the synaptic stripper. Neuron *77*, 10–18.

Knapp, L.T., and Klann, E. (2002). Potentiation of hippocampal synaptic transmission by superoxide requires the oxidative activation of protein kinase C. J. Neurosci. *22*, 674–683.

Loiarro, M., Sette, C., Gallo, G., Ciacci, A., Fantò, N., Mastroianni, D., Carminati, P., and Ruggiero, V. (2005). Peptide-mediated interference of TIR domain dimerization in MyD88 inhibits interleukin-1-dependent activation of NF-kappaB. J. Biol. Chem. *280*, 15809–15814.

Maalouf, M., and Rho, J.M. (2008). Oxidative impairment of hippocampal long-term potentiation involves activation of protein phosphatase 2A and is prevented by ketone bodies. J. Neurosci. Res. *86*, 3322–3330.

Mann, D.A., and Frankel, A.D. (1991). Endocytosis and targeting of exogenous HIV-1 Tat protein. EMBO J. *10*, 1733–1739.

Mulkey, R.M., Herron, C.E., and Malenka, R.C. (1993). An essential role for protein phosphatases in hippocampal long-term depression. Science *261*, 1051–1055.

Nicholls, R.E., Alarcon, J.M., Malleret, G., Carroll, R.C., Grody, M., Vronskaya, S., and Kandel, E.R. (2008). Transgenic mice lacking NMDAR-dependent LTD exhibit deficits in behavioral flexibility. Neuron *58*, 104–117.

Nimmerjahn, A., Kirchhoff, F., and Helmchen, F. (2005). Resting microglial cells are highly dynamic surveillants of brain parenchyma in vivo. Science *308*, 1314–1318.

Nizet, V., and Johnson, R.S. (2009). Interdependence of hypoxic and innate immune responses. Nat. Rev. Immunol. *9*, 609–617.

Nolan, Y., Martin, D., Campbell, V.A., and Lynch, M.A. (2004). Evidence of a protective effect of phosphatidylserine-containing liposomes on lipopolysaccharide-induced impairment of long-term potentiation in the rat hippocampus. J. Neuroimmunol. *151*, 12–23.

Peers, C., Dallas, M.L., Boycott, H.E., Scragg, J.L., Pearson, H.A., and Boyle, J.P. (2009). Hypoxia and neurodegeneration. Ann. N Y Acad. Sci. *1177*, 169–177.

Pei, Z., Pang, H., Qian, L., Yang, S., Wang, T., Zhang, W., Wu, X., Dallas, S., Wilson, B., Reece, J.M., et al. (2007). MAC1 mediates LPS-induced production of superoxide by microglia: the role of pattern recognition receptors in dopaminergic neurotoxicity. Glia *55*, 1362–1373.

Pi, H.J., and Lisman, J.E. (2008). Coupled phosphatase and kinase switches produce the tristability required for long-term potentiation and long-term depression. J. Neurosci. *28*, 13132–13138.

Qin, L., Liu, Y., Wang, T., Wei, S.J., Block, M.L., Wilson, B., Liu, B., and Hong, J.S. (2004). NADPH oxidase mediates lipopolysaccharide-induced neurotoxicity and proinflammatory gene expression in activated microglia. J. Biol. Chem. *279*, 1415–1421.

Raddatz, E., Thomas, A.C., Sarre, A., and Benathan, M. (2011). Differential contribution of mitochondria, NADPH oxidases, and glycolysis to region-specific oxidant stress in the anoxic-reoxygenated embryonic heart. Am. J. Physiol. Heart Circ. Physiol. *300*, H820–H835.

Relman, D., Tuomanen, E., Falkow, S., Golenbock, D.T., Saukkonen, K., and Wright, S.D. (1990). Recognition of a bacterial adhesion by an integrin: macrophage CR3 (alpha M beta 2, CD11b/CD18) binds filamentous hemagglutinin of Bordetella pertussis. Cell *61*, 1375–1382.

Rey, F.E., Cifuentes, M.E., Kiarash, A., Quinn, M.T., and Pagano, P.J. (2001). Novel competitive inhibitor of NAD(P)H oxidase assembly attenuates vascular O(2)(-) and systolic blood pressure in mice. Circ. Res. *89*, 408–414.

Reynolds, A., Laurie, C., Mosley, R.L., and Gendelman, H.E. (2007). Oxidative stress and the pathogenesis of neurodegenerative disorders. Int. Rev. Neurobiol. *82*, 297–325.

Rius, J., Guma, M., Schachtrup, C., Akassoglou, K., Zinkernagel, A.S., Nizet, V., Johnson, R.S., Haddad, G.G., and Karin, M. (2008). NF-kappaB links innate immunity to the hypoxic response through transcriptional regulation of HIF-1alpha. Nature *453*, 807–811.

Schafer, D.P., Lehrman, E.K., Kautzman, A.G., Koyama, R., Mardinly, A.R., Yamasaki, R., Ransohoff, R.M., Greenberg, M.E., Barres, B.A., and Stevens, B. (2012). Microglia sculpt postnatal neural circuits in an activity and complement-dependent manner. Neuron *74*, 691–705.

Schwarze, S.R., Hruska, K.A., and Dowdy, S.F. (2000). Protein transduction: unrestricted delivery into all cells? Trends Cell Biol. *10*, 290–295.

Sheth, P., Samak, G., Shull, J.A., Seth, A., and Rao, R. (2009). Protein phosphatase 2A plays a role in hydrogen peroxide-induced disruption of tight junctions in Caco-2 cell monolayers. Biochem. J. *421*, 59–70.

Stephan, A.H., Barres, B.A., and Stevens, B. (2012). The complement system: an unexpected role in synaptic pruning during development and disease. Annu. Rev. Neurosci. *35*, 369–389.

Stevens, B., Allen, N.J., Vazquez, L.E., Howell, G.R., Christopherson, K.S., Nouri, N., Micheva, K.D., Mehalow, A.K., Huberman, A.D., Stafford, B., et al. (2007). The classical complement cascade mediates CNS synapse elimination. Cell *131*, 1164–1178.

Trevelyan, A.J., Sussillo, D., Watson, B.O., and Yuste, R. (2006). Modular propagation of epileptiform activity: evidence for an inhibitory veto in neocortex. J. Neurosci. *26*, 12447–12455.

von Lubitz, D.K. (1999). Adenosine and cerebral ischemia: therapeutic future or death of a brave concept? Eur. J. Pharmacol. *371*, 85–102.

Wake, H., Moorhouse, A.J., Jinno, S., Kohsaka, S., and Nabekura, J. (2009). Resting microglia directly monitor the functional state of synapses in vivo and determine the fate of ischemic terminals. J. Neurosci. *29*, 3974–3980.

Wake, H., Moorhouse, A.J., Miyamoto, A., and Nabekura, J. (2013). Microglia: actively surveying and shaping neuronal circuit structure and function. Trends Neurosci. *36*, 209–217.

Wright, S.D., and Jong, M.T. (1986). Adhesion-promoting receptors on human macrophages recognize Escherichia coli by binding to lipopolysaccharide. J. Exp. Med. *164*, 1876–1888.

Yang, M., and Kahn, A.M. (2006). Insulin-stimulated NADH/NAD+ redox state increases NAD(P)H oxidase activity in cultured rat vascular smooth muscle cells. Am. J. Hypertens. *19*, 587–592.

Zhang, W., Dallas, S., Zhang, D., Guo, J.P., Pang, H., Wilson, B., Miller, D.S., Chen, B., Zhang, W., McGeer, P.L., et al. (2007). Microglial PHOX and Mac-1 are essential to the enhanced dopaminergic neurodegeneration elicited by A30P and A53T mutant alpha-synuclein. Glia *55*, 1178–1188.

Zhang, D., Hu, X., Qian, L., Chen, S.H., Zhou, H., Wilson, B., Miller, D.S., and Hong, J.S. (2011). Microglial MAC1 receptor and PI3K are essential in mediating β-amyloid peptide-induced microglial activation and subsequent neurotoxicity. J. Neuroinflammation *8*, 3.

Zlokovic, B.V. (2011). Neurovascular pathways to neurodegeneration in Alzheimer's disease and other disorders. Nat. Rev. Neurosci. *12*, 723–738.